Abdominal Wall CT Angiography: A Detailed Account of a Newly Established Preoperative Imaging Technique[1]

Timothy J. Phillips, MBBS, GradDipSurgAnat
Damien L. Stella, MBBS, FRANZCR
Warren M. Rozen, MBBS, BMedSci, PGDipSurgAnat
Mark Ashton, MBBS, MD, FRACS
G. Ian Taylor, MBBS, MD, FRCS, FRACS, AO

Institutional review board approval was obtained for this study, and all patients gave written informed consent. Autologous surgical breast reconstruction with use of abdominal wall donor flaps based on the deep inferior epigastric artery (DIEA) and one or more of its anterior musculocutaneous perforating branches (DIEA perforator flap) is being used with increasing frequency instead of breast reconstruction with use of traditional transverse rectus abdominus musculocutaneous and modified muscle-sparing flaps. Preoperative mapping of the DIEA perforators with abdominal wall computed tomographic (CT) angiography may improve patient care by providing the surgeon with additional information that will lead to optimization of the surgical technique, shorter procedure time, and reduction in the frequency of surgical complications. The branching patterns of the DIEA, the segmental anatomy of the anterior adipocutaneous perforating branches of the DIEA, and the importance of these features in pre- and intraoperative surgical planning necessitate a different approach to abdominal wall CT angiography than that used with other abdominal CT angiographic techniques. In abdominal wall CT angiography, the common femoral artery is used as the bolus trigger, CT scanning is performed in the caudocranial direction, the automatic exposure control feature is disabled, a scaled grid overlay tool is used to present information to the surgeons, and radiation dose is minimized (average dose, 6 mSv). The anatomic accuracy of abdominal wall CT angiography has been investigated in cadaveric and surgical studies, with sensitivity of 96%–100% and specificity of 95%–100%. This detailed description will allow other radiologists and surgeons interested in free DIEP flap surgery to incorporate this useful tool into their practice.

Supplemental material: *http://radiology.rsnajnls.org/cgi/content/full/249/1/32/DC1*

[1] From the Department of Radiology, the Royal Melbourne Hospital, Grattan Street, Parkville, Melbourne, Victoria 3050, Australia. Received November 26, 2007; revision requested January 15, 2008; revision received March 21; final version accepted April 3. **Address correspondence to** T.J.P. (e-mail: *timothy.john.phillips@gmail.com*).

Radiology

Autologous surgical breast reconstruction with abdominal wall donor flaps has evolved since its introduction in the late 1970s and early 1980s (1,2). Free flaps based on the deep inferior epigastric artery (DIEA) and one or more of its anterior musculocutaneous perforating branches (hereafter, perforators) are termed DIEA perforator flaps, and they are being used with increasing frequency to replace the traditional transverse rectus abdominus musculocutaneous flaps and the modified muscle-sparing flaps (3–6). The DIEA perforator flap is used to harvest fat and skin (adipocutaneous tissue) without muscle and has resulted in fewer abdominal wall complications—including hernia, bulge, and weakness (3,7–10)—and shorter hospital stays, with a cheaper overall cost of treatment (11,12) when compared with alternative surgical techniques. The superficial inferior epigastric artery can also be used for an adipocutaneous muscle-sparing flap, and it is the preferred surgical option for an abdominal wall free flap, as it does not require incision of the anterior rectus sheath and thus has minimal donor site morbidity (13,14). However, this vessel is not uniformly present or of sufficient caliber to perform the operation.

The branching pattern of the DIEA and the location of its perforators vary, and each patient's anatomy dictates the DIEA and perforator(s) on which the flap will be based (15,16). Preoperative Doppler ultrasonography (US) is useful when defining the DIEA branching pattern; however, locating and choosing the perforators was previously complete only after intraoperative abdominal wall dissection. Identification of optimal perforators on which to base the flap is highly desirable. There is evidence that flaps based on fewer perforators have a lower incidence of fat necrosis (7). Harvesting a flap supplied by one perforator requires the identification of a perforator with optimal characteristics (discussed in detail later in this article).

Abdominal wall computed tomographic (CT) angiography is a new technique tailored to assist in locating and characterizing the perforators, with reported sensitivity and specificity of 96%–100% and 95%–100%, respectively, in cadaveric and clinical studies (17–23). In addition, this technique can be used to define the branching pattern of the DIEA (18,23). The intent of this article is to provide those who are interested in abdominal wall CT angiography with a step-by-step manual that describes our approach to this modality. Included are considerations regarding appropriate patient selection, contrast material enhancement, image acquisition and reconstruction parameters, image display and analysis techniques, and the radiology report, which includes the presentation of data to the referring surgeon. An explanation of the surgical and radiologic anatomy of the DIEA and the characteristics that define favorable perforators is also included. These recommendations are based on the authors' experience in performing and interpreting the results of 65 abdominal wall CT angiographic examinations and on close collaboration between the departments of radiology and plastic surgery at our institution.

Essentials

- We have detailed the use of radiologic classification of the segmental anatomy of the anterior musculocutaneous perforating branches (hereafter, perforators) of the deep inferior epigastric artery (DIEA) and the surgical relevance of this classification for free adipocutaneous flap harvest.
- We have developed a CT angiography acquisition technique optimized for imaging the DIEA and the anterior musculocutaneous branches (perforators) supplying the abdominal wall.
- We have described CT angiography postprocessing techniques optimized for display of the surgically relevant findings.
- We have demonstrated a volume-rendering color look-up table optimized for imaging of anterior musculocutaneous branches of the DIEA in the subcutaneous fat of the abdominal wall.
- We have demonstrated a real-time volume-rendered image manipulation reading technique that enables preoperative mapping of DIEA perforators.
- Autologous breast reconstruction with use of adipocutaneous free flaps (DIEA perforator flap) is the optimal standard of care after mastectomy.
- Preoperatively mapping DIEA perforators with this abdominal wall CT angiography technique may improve patient care by providing the surgeon with additional information that leads to optimization of the surgical technique, shorter operative time, and a reduction in the frequency of operative complications.

Anatomy

DIEA Classification

Cadaveric and surgical studies have been performed to classify the branching pattern of the DIEA. The branching classification first described by Moon and Taylor has been widely adopted and is shown in Figure 1 (15). In addition to the major branching patterns (types I, II, and III) of the DIEA above the arcuate line, early branches also include a pubic branch, muscular branches, and an umbilical branch (15).

Type I (single trunk) and type II (bifurcation into two trunks) branching patterns occur more commonly than does the type III pattern (division into more than two trunks). The other relevant characteristics are the caliber of the trunk(s) and any intramuscular

Published online
10.1148/radiol.2483072054

Radiology 2008; 249:32–44

Abbreviations:
CLUT = color look-up table
DIEA = deep inferior epigastric artery
MIP = maximum intensity projection
VRT = volume-rendered technique

Authors stated no financial relationship to disclose.

course. Usually, the DIEA enters the rectus sheath superficial to the arcuate line and courses superiorly between the posterior layer of the rectus sheath and the rectus muscle. It is not uncommon for one or both of the DIEAs to penetrate and course within the rectus muscle for some part of their length (15,24,25).

Segmental Arterial Anatomy of DIEA Perforators

The descriptions and nomenclature applied to the variations in perforator anatomy in cadaveric studies and surgical observations are diverse, but the key findings are similar (24–26). The course a perforator takes from its origin at the DIEA through four anatomic spaces to its end supply of the subcutaneous fat and skin of the anterior abdominal wall is shown in Figure 2. We refer to the portions of each perforator defined by the anatomic spaces as segments (Figs 2, 3). Perforators originate from the DIEA, which is usually located between the posterior layer of the rectus sheath and the posterior border of the rectus muscle. The perforator penetrates the posterior surface of the rectus abdominus and has a variable intramuscular segment. In cases where the artery penetrates a musculotendinous intersection, the intramuscular segment may be absent. Often, this segment penetrates the anterior surface of the rectus sheath and the anterior layer of the fascial sheath simultaneously; however, it can alternatively have a varying subfascial segment between the anterior border of the rectus muscle and the anterior layer of the rectus sheath. The course and branching of the subcutaneous segment within the subcutaneous fat is variable and involves varying anastomoses with the superficial inferior epigastric artery. Perforators originating from type II DIEAs are often arranged in two rows along the course of each trunk. Some authors refer to these as medial and lateral row perforators. In addition, some authors refer to perforators that penetrate the anterior rectus sheath near the umbilicus and supply the adjacent subcutaneous fat as

Figure 1

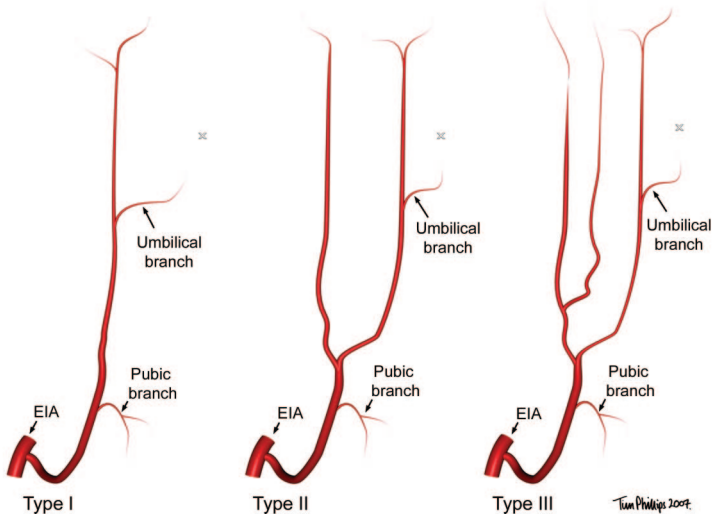

Figure 1: Three-dimensional graphic illustrations show the classification of DIEA branching described by Moon and Taylor (15). Type I (single trunk) and type II (bifurcation into two trunks) branching are more common than type III branching (division into more than two trunks). The umbilical and descending pubic branches are seen regularly. The level of the umbilicus (×) is indicated on each illustration. *EIA* = external iliac artery.

Figure 2

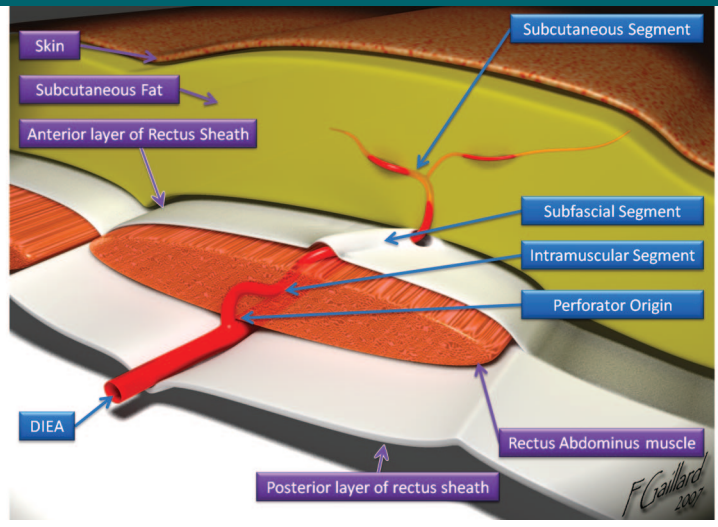

Figure 2: Three-dimensional graphic illustration of the course of a perforator (anterior musculocutaneous branch) from its origin at the DIEA between the posterior layer of the rectus sheath and the rectus muscle, its intramuscular segment within the rectus muscle, its subfascial segment (not always present) between the anterior aspect of the rectus muscle and the anterior layer of the rectus sheath, and its end branching (subcutaneous segment) within the subcutaneous fat of the anterior abdominal wall. (Image courtesy of Francesco Gaillard, MBBS, Royal Melbourne Hospital, Australia.)

Figures 3, 4

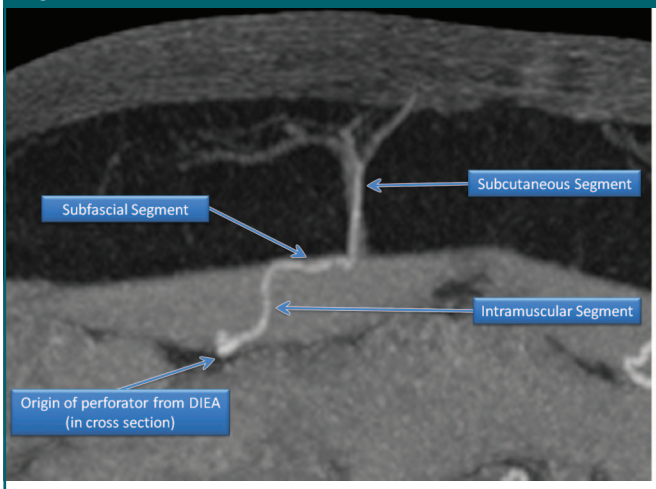

Figure 3: Axial 50-mm section thickness maximum intensity projection (MIP) image obtained with abdominal wall CT angiography shows the labeled segments of a perforator originating from the right DIEA.

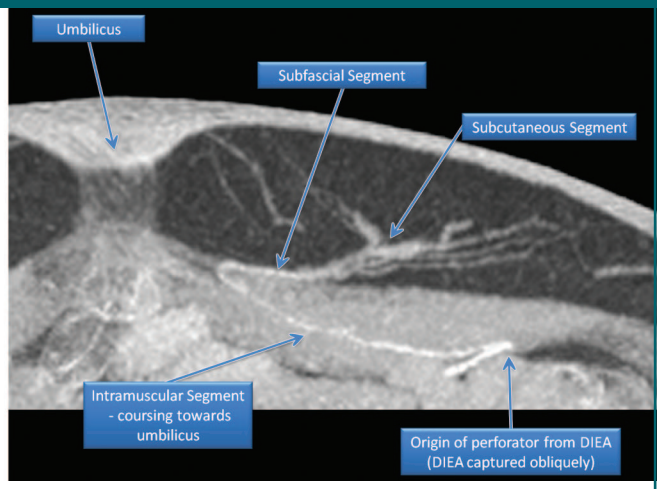

Figure 4: Axial 50-mm section thickness MIP image shows a perforator with a long intramuscular segment coursing medially toward the umbilicus. The subfascial and subcutaneous segments course away from the umbilicus. Some authors refer to these as paraumbilical perforators or paramedian perforators.

Table 1

Relevant Characteristics of the Arteries of the Anterior Abdominal Wall and Their Importance to DIEA Perforator Flap Surgery

Abdominal Wall Artery	Relevant Characteristic	Importance to DIEA Perforator Surgery
DIEA	Caliber	A large-caliber trunk is a more favorable pedicle.
DIEA	Branching pattern (type I, II, or III)	The DIEA branch forms the pedicle for the anastomosis. Type I and type II arteries have perforators with shorter intramuscular segments. Type II arteries often have perforators arranged in rows along each trunk; two or more of these perforators may be dissected to a single trunk. Type II and type III arteries have a lateral branch that is in the vicinity of the motor nerves to the rectus abdominus; dissection of this branch raises the risk of muscle denervation.
DIEA	Any intramuscular course	Any intramuscular course makes dissection of the DIEA more difficult.
DIEA perforator		
Intramuscular perforator	Direction and length	Oblique intramuscular segments require more dissection of the rectus abdominus. Perforators that penetrate a musculotendinous intersection may not have an intramuscular segment and are preferred by some surgeons.
Subfascial perforator	Length and direction	Radiologically, the subfascial segment origin can be confused with the subcutaneous segment origin. Long subfascial segments require careful dissection to preserve the perforator when incising the rectus sheath.
Subcutaneous perforator	Location and caliber	Large-caliber (≥1 mm in diameter) arteries supply a greater volume of adipocutaneous tissue and represent better vascular pedicles. Preoperative knowledge of the subcutaneous segment origin facilitates accurate planning of dissection.
Superficial inferior epigastric artery	Caliber and location	Use of a large-caliber superficial inferior epigastric artery as a vascular pedicle for a free flap is favored by some surgeons.

Table 2

Acquisition Parameters

Parameter	Somatom Sensation 64	Somatom Sensation 16
Collimation (mm)	64 × 0.6	16 × 0.75
Helical beam pitch	0.9	1.13
Tube voltage (kV)	120	120
Tube current (mAs)	180–200	180–200
Rotation time (sec)	0.37	0.5
Reconstruction section thickness (mm)	0.75	1
Reconstruction section spacing (mm)	0.4	0.7

Table 3

Reconstruction and Image Display Methods Used in Abdominal Wall CT Angiography

Reconstruction Method	Image Display Method
Reconstruction generated automatically at CT scanner workstation	Thin overlapping 0.75/0.4 mm axial images, thick contiguous 20/20 mm MIP images, or thick overlapping 50/20 mm MIP images*
Reconstruction generated at CT scanner workstation by imaging technologist	Coronal MIP image with voxels cut away to demonstrate the DIEA branching pattern
Reconstruction manipulated in real time at reporting workstation by reading radiologist	VRT images or multiplanar reformation images
Reconstructions created at reporting workstation by the radiologist for presentation to the surgeon	VRT reconstructed abdominal wall images with perforators marked or coronal MIP images with perforators marked

Note.—VRT = volume-rendered technique.

* To ensure the entire course of each perforator is captured on one image, both thick contiguous MIPs and thick overlapping MIPs are created. The thick overlapping MIPs are used only when the entire course of a perforator is not evident on the thick contiguous MIPs, as these images contain many overlapping vessels.

paraumbilical or paramedian perforators, an example of which is shown in Figure 4.

Important Anatomic Features for DIEA Perforator Flap Surgery

Table 1 details the relevant characteristics of the DIEA, the segments of the perforators, and the superficial inferior epigastric artery. Both type I and type II branching patterns have been shown to have perforators that have a shorter intramuscular course than do perforators in patients with type III branching patterns (20). Individual perforators can be traced to individual branches, and the branch forms the pedicle for the anastomosis. A type II or type III branching pattern has a lateral branch that is in the vicinity of the motor nerves to the rectus abdominus. Leaving this lateral branch in situ by removing a medial branch only leaves those nerves undisturbed. Denervation of the rectus abdominus defeats the purpose of a muscle-sparing adipocutaneous flap and is highly undesirable. Preoperative knowledge of the DIEA branching pattern may therefore aid the surgeon's choice of which perforator to use and the hemiabdomen of choice.

Perforator anatomy is used to determine the surgeon's choice of perforator(s) on which to base a DIEA perforator flap, and it influences surgical planning and technique (20,21,26). A large-caliber (≥1 mm in diameter) perforator with a large subcutaneous segment will supply a larger volume of adipocutaneous tissue. Perforators with a subcutaneous segment origin that is at a musculotendinous intersection are preferred by some surgeons and anecdotally have shorter (or absent) intramuscular and subfascial segments. Knowledge of the subfascial segment (if any) is desirable, as these segments require careful dissection. A

Figure 5

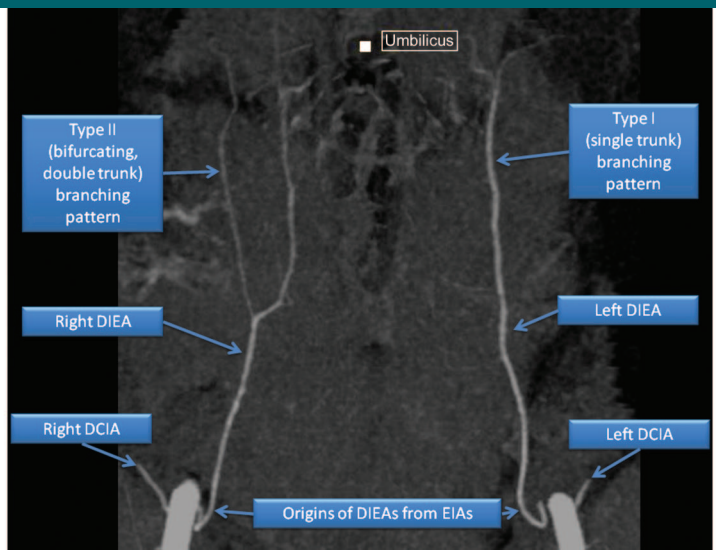

Figure 5: Coronal MIP image with voxels cut away from the three-dimensional dataset to optimize display of the branching pattern of the DIEAs from their origins at the external iliac arteries *(EIAs)*. The right DIEA has a type II pattern, and the left DIEA has a type I pattern. The umbilicus is visible. The deep circumflex iliac artery *(DCIA)* can also be seen branching from the external iliac arteries.

long intramuscular segment with a substantial lateral or medial component to its course requires more dissection of the rectus muscle. Extensive rectus muscle dissection is not desired and theoretically increases abdominal wall morbidity. A more medial perforator means that dissection through the rectus muscle is less likely to denervate the muscle that receives its nerve supply laterally. Denervation of the rectus muscle negates the abdominal wall morbidity benefits of the DIEA perforator flap technique and is highly undesirable. A row of perforators in a sagittal plane originating from the same DIEA trunk is favorable for surgeons who prefer to base DIEA perforator flaps on more than one perforator, as the rectus muscle can be split in a sagittal plane to dissect these vessels to their origin.

Patient Selection

Planned autologous breast reconstruction with use of an abdominal wall donor flap is an indication for abdominal wall CT angiography. The technique may also be performed for other planned abdominal wall flap–based reconstructions, such as those that use the superficial inferior epigastric artery, deep circumflex iliac artery, or superficial circumflex iliac artery. The only absolute contraindication is a previous anaphylactic reaction to intravenous iodinated contrast material. Severe renal impairment may also preclude the use of intravenous iodinated contrast material.

Image Acquisition

Patient Positioning and Preparation

Ideally, patients undergo imaging in the supine position, as this mimics the intraoperative position. It is important for patients to not wear clothing that deforms the contour of the abdominal wall. This includes the patient's own clothing, as well as any strings attached to hospital gowns. The Velcro straps (which may compress the abdominal wall and force the patient's clothing to lie close to her skin) ensure stable patient position and prevent the patient from falling from the CT scanner table. These straps are placed outside the scanning range to optimize subsequent image reconstruction.

Acquisition Volume and Range

The superior extent of the tissue volume to be characterized is the superior limit of the planned (donor site) surgical field. This is a point 3–4 cm above the umbilicus. The inferior extent is the origin of the superficial inferior epigastric artery from the common femoral artery.

Contrast Material Enhancement and Scanning Direction

The DIEA and superficial inferior epigastric artery fill from the external iliac and common femoral arteries, respectively, in a caudocranial direction. Thus, contrast material enhancement of the inferior epigastric vessels is optimized by timing the CT acquisition with use of bolus tracking at the common femoral artery rather than at the aorta and scanning in a caudocranial direction. A total of 100 mL of an intravenous, low-osmolar, nonionic iodinated high-concentration (350–370 mg/mL) contrast agent is administered with a dual-chamber injection pump at a rate of 4 mL/sec and immediately followed by a 50-mL saline bolus flush administered at a rate of 4 mL/sec. For the suggested injection rate, the choice of high-concentration (>350 mg/mL) monomeric iodinated contrast material may aid in the identification of tiny perforator branches, particularly intramuscular segments. The evidence for this possibility comes from literature in which researchers evaluated visualization of small vessels supplying the brain, heart, pancreas, liver, and lungs (27–31). Alternately,

Figure 6

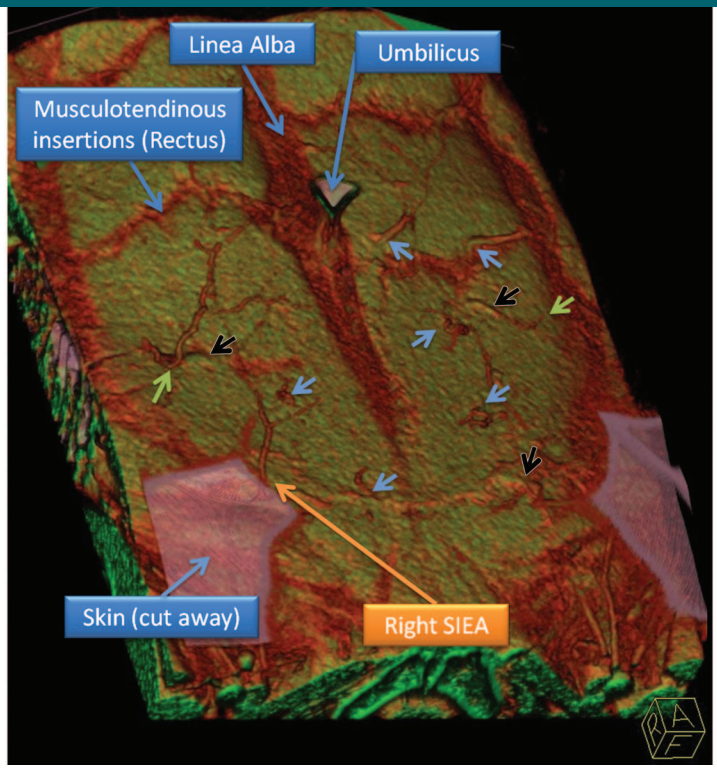

Figure 6: Oblique VRT image obtained with use of our customized CLUT to optimize visualization of the anterior rectus sheath, the subfascial and subcutaneous segments of the perforators, the musculotendinous insertions, and the superficial inferior epigastric artery *(SIEA)*. Small blue arrows = perforators that emerge from the sheath without a substantial subfascial segment, black arrows = subfascial segments, green arrows = subcutaneous segments of perforators with subfascial segments.

Figure 7

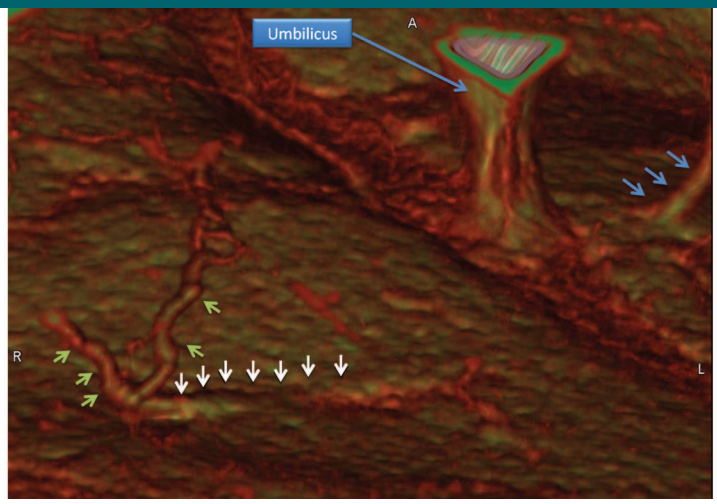

Figure 7: Oblique close-up VRT image shows the subfascial (white arrows) and subcutaneous (yellow-green arrows) segments of a right-sided perforator. The proximal subcutaneous segment (blue arrows) of a left-sided perforator is also visible.

Figure 8

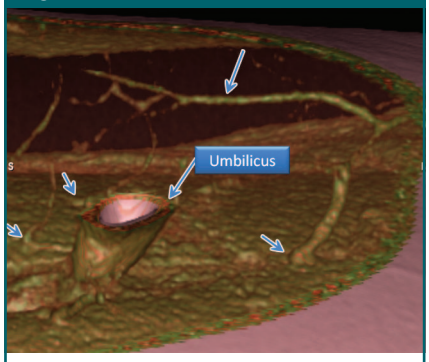

Figure 8: Screen-capture image obtained during real-time manipulation of a VRT image, as seen from the right side of the body. The umbilicus, several perforators (short arrows), and a large left-sided superior-inferior epigastric artery (long arrow) are visible.

Figure 9

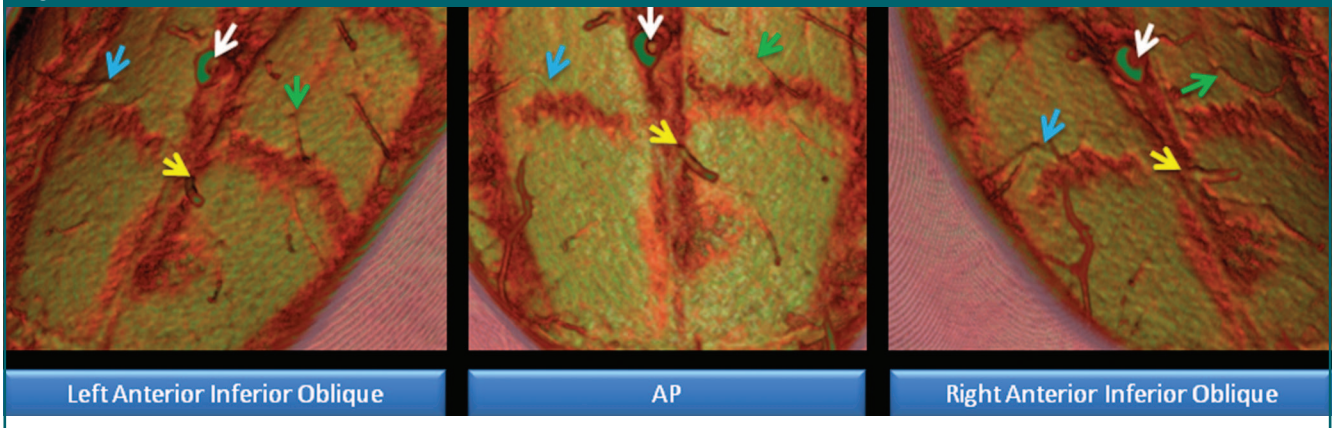

Figure 9: Screen-capture images obtained during real-time manipulation of a VRT image, with volume cropping in a coronal-frontal orientation. The umbilicus (white arrow) and three large perforators (blue, yellow, and green arrows) are visible. Three perspectives (left anterior inferior oblique, anteroposterior *[AP],* and right anterior inferior oblique) of the same cropped volume with the same perforators marked are shown to demonstrate the benefit of real-time image manipulation. Note the subfascial course of the perforator indicated by the blue arrow is more apparent on the anteroposterior and right anterior inferior oblique images.

use of a monomeric iodinated contrast agent with a concentration of 300 mg/mL and an injection rate of 5 mL/sec should produce equivalent vascular attenuation results. The trigger for acquisition is attenuation of the common femoral artery to a level of more than 100 HU at the axial level of the pubic symphysis. This level also provides a bone landmark for the inferior limit of the scan volume in the z-axis. Acquisition begins with the minimum delay achievable, typically 4 seconds, on modern multidetector CT scanners.

Acquisition Parameters

Contiguous isometric acquisition data obtained with thin-collimation helical CT are ideal for quality CT angiography. On the multidetector CT scanners (Somatom Sensation 16 and Somatom Sensation 64; Siemens Medical Solutions, Erlangen, Germany) used to perform abdominal wall CT angiographic examinations, we used settings that balanced low radiation dose with good image quality; this is known as the ALARA (as low as reasonably achievable) principle (Table 2). Diagnostic-quality images were obtained with both scanners. Use of

120-kV tube voltage and 180–200-mAs tube current results in high-quality images and acceptable effective dose estimates for the limited scanning range of abdominal wall CT angiography. With this technique, the effective dose is 6 mSv for an average-sized patient with a scanning range of 30 cm (ImPACT CT Patient Dosimetry Calculator, version 0.99w; St George's Hospital, London, England). Automatic exposure control was notable for its absence from our scanning protocol.

Modern multidetector CT scanners have software that can be used to modulate tube current in two axes. Modulation in the z-axis based on the varying shape of the patient and angular modulation is adjusted in real time with a single gantry rotation delay (32). When we compared abdominal wall CT angiography performed with dose modulation enabled with abdominal wall CT angiography performed with dose modulation disabled, we found that disabling dose modulation resulted in a similar dose estimate and, subjectively, less image noise in the abdominal wall (therefore enabling better visualization of the tiny perforator branches, particularly the intramuscular segments). The dose estimate was determined by evaluating effective dose in an average-sized patient who underwent imaging with dose modulation enabled and subsequently calculating the effective dose had dose modulation been disabled. Both techniques resulted in a dose of 6 mSv. The similar dose estimate is not surprising, as the scanning range almost entirely covered the bony pelvis, where dose modulation techniques had little effect in reducing dose. Image quality was judged subjectively by comparing side-by-side studies of patients with similar body habitus and scanning protocols but with dose modulation enabled or disabled. It is assumed that the perceived improvement in image quality could have been caused by the angular modulation algorithms, which were designed to optimize signal-to-noise ratio in the intraabdominal region of the images rather than in the abdominal wall (32).

Figure 10

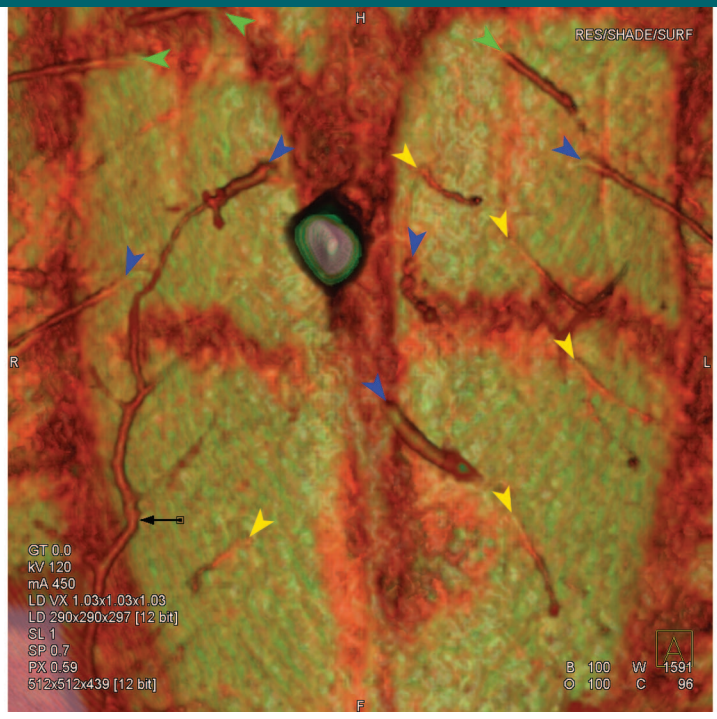

Figure 10: Step 1 of surgical map creation. VRT image seen from the coronal-frontal perspective with the skin cropped to reveal subcutaneous segments of the perforators. This same image is used for Figures 11 and 12. The radiologist marks perforators (arrowheads) at the point that they penetrate the anterior rectus sheath. Blue arrowheads indicate a large (≥1.0 mm diameter) perforator; yellow arrowheads, a small perforator (<1.0 mm diameter); and green arrowheads, perforators superior to the umbilicus that are not surgically relevant. A large superficial inferior epigastric artery is also seen (arrow). The umbilicus skin is visible in the middle of the image.

Image Reconstruction

In our clinical practice of abdominal wall CT angiography, all image reconstruction is performed at a Leonardo (Siemens Medical Solutions) workstation equipped with imaging software (Syngo 3D VRT and Syngo InSpace 4D, version 2006A; Siemens Medical Solutions). The images in this article (except when stated otherwise) were created at this same workstation with the same imaging software. None of the tools used in this study—including the grid overlay tool—is vendor specific, and all are available on all CT workstations endorsed by major vendors. Table 3 lists the image reconstruction and display methods used. Thin overlapping axial images and thick MIP axial images are preprogrammed into the CT scanning protocol for automatic reconstruction at the scanner console. The thin overlapping axial images are used as image data for multiplanar reformations, as well as to generate the MIP and VRT images created by the technologist and radiologist. Experienced technologists spend an average of 10 minutes per patient on image reconstruction. The reporting radiologist (D.L.S.) spends an average of 7 minutes per patient on image reconstruction. Given the usual course of DIEAs, the image data effectively provide images in the transaxial plane in most patients and are therefore used to measure the caliber of the DIEAs, as various in vivo and in vitro studies have shown the use of MIPs and multiplanar reformations alone is prone to inaccuracy in vascular imaging (33–36).

We prefer to use thick axial MIP images to demonstrate the intramuscular and subcutaneous segments of the perforators. Figure 3 is a 50-mm axial MIP image obtained with abdominal

wall CT angiography that shows the intramuscular, subfascial, and subcutaneous segments of a perforator and its origin from the right DIEA.

Certain subtypes of perforators described by some authors are well demonstrated on thick axial MIP images. Figure 4 shows a perforator with a long intramuscular segment coursing medially toward the umbilicus. The subfascial and subcutaneous segments course away from the umbilicus. Various authors refer to these as paraumbilical or paramedian perforators (24,26). When present, this perforator is often a continuation or branch of the umbilical branch of the DIEA. As discussed previously, a long intramuscular segment is an unfavorable characteristic.

Coronal MIP images are obtained to determine the branching pattern of DIEAs. Figure 5 is an MIP image that shows a type II DIEA branching pattern on the left side of the image and a type I pattern on the right side of the image. These images were created by the medical imaging technologist at a CT workstation. The cut-away feature of the workstation can be used to remove parts of the volume anterior (skin) and posterior (omental and/or mesenteric arteries and enhancing bowel wall) to the region of interest to better depict the DIEA course.

VRT is an image display technique that is used to assign color and opacity values to voxels and display a two-dimensional representation of the three-dimensional dataset. Additional features and graphics-processing methods vary between software vendors. Common to all VRT software is the color look-up table (CLUT), which is used to assign voxel color and opacity on the basis of CT numbers. We have developed a CLUT that optimally displays the subfascial segments of the perforators, the location at which perforators pass through the anterior rectus sheath, and the branching and caliber of the subcutaneous segments. This CLUT is designed to make the subcutaneous fat completely transparent and maximize the surface contours of the anterior rectus sheath and the subfascial and subcutaneous segments of the perforators. The skin has a range of attenuations that overlaps with that of the rectus sheath and the perforators. The CLUT is designed to color the skin pink, which allows these structures to be distinguished from each other, and adds realistic surface rendering of the abdominal wall skin for the images presented to the surgeons. We have developed working CLUTs for both Syngo InSpace 4D software and OsiriX open-source software *(http://www.osirix-viewer.com/)* distributed under the GNU general public license.

VRT images obtained with our CLUT are optimized for visualization of the subcutaneous and subfascial segments of the perforators. The shiny green surface of the anterior rectus sheath demonstrates the contour of the subfascial segments, and the red-green surface shading of the subcutaneous segments is highlighted against the transparent fat (Fig 6). The musculotendinous insertions appear red against the green surface of the remainder of the anterior rectus sheath. This is the only image format in which the musculotendinous insertions are delineated as being separate from the muscular rectus. Figure 7 is a close-up image acquired with VRT that highlights the subfascial and subcutaneous segments of a perforator. Figure 8 demonstrates the ability of the OsiriX software to perform this function with a similarly customized VRT CLUT.

Real-time manipulation of the VRT display involves use of volume cropping and clip planes by the radiologist to facilitate mapping of the locations of the points at which the perforators penetrate the anterior rectus sheath and any subfascial segments. The radiologist uses this method to ultimately construct a scaled map that the surgeon uses intraoperatively.

With use of a VRT image viewed from an anterior anatomic coronal perspective (effectively viewing the

Figure 11

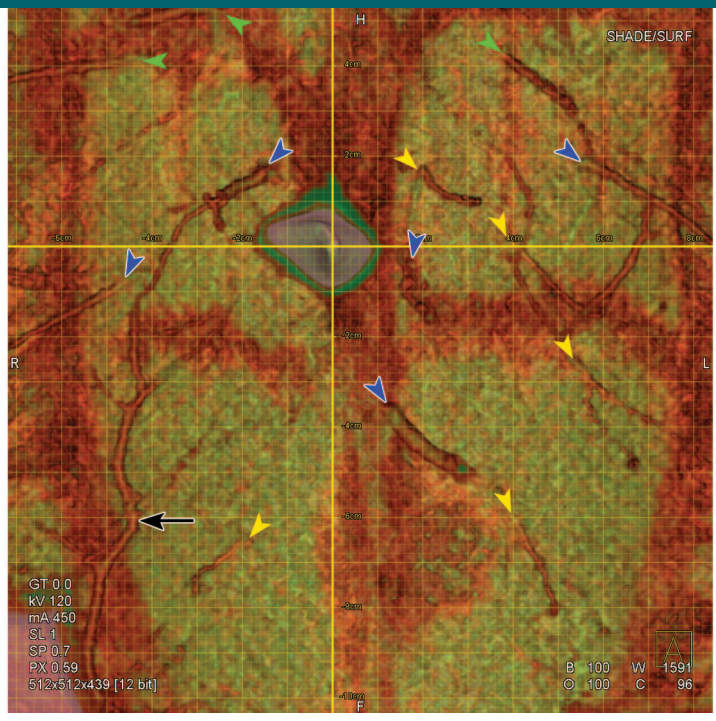

Figure 11: Step 2 of surgical map creation. A grid is overlaid to facilitate measurement of the subcutaneous perforator origins in orthogonal axes from the umbilicus.

abdominal wall from in front), an anterior coronal clip plane, volume cropping, or both are used to cut away the skin and varying amounts of subcutaneous fat to survey the anterior rectus sheath and locate the point at which the perforators penetrate the anterior rectus sheath. Identification of the critical anatomy is also aided by rotating the VRT image into the perspective most suitable (usually much closer to a view perpendicular to the surface of the abdominal wall) to verify that a suspected perforator is a real finding (Fig 9).

The steps the radiologist takes to create the final images for presentation to the surgeon are outlined sequentially in Figures 10–13. The radiologist uses arrows to mark perforators (Fig 10), with color coding used to denote large (≥1.0 mm diameter) and small (<1.0 mm diameter) perforators. It is ensured that the VRT image is restored to the original scanning orientation when the arrowheads are placed to avoid misregistration artifacts that may result from the multiple VRT rotations that occur during the mapping process. These arrowheads are located outside the VRT volume, so they do not inadvertently move during image manipulation. A scaled grid is applied to the image with the 0,0 point of the axis at the umbilicus (Fig 11). The clip plane is removed, leaving a surface-rendered view of the anterior abdominal wall, with the arrowheads still marking the location of the perforators (Fig 12). This is one of the images the surgeon uses intraoperatively. The same grid and arrowheads are overlaid onto the coronal MIP image previously described (Fig 13). This single image facilitates a spatial appreciation of the relationship between the perforators and their parent DIEA trunks, allowing the surgeon to easily identify large perforators that have long oblique intramuscular or subfascial segments. Two movies demonstrating this process in real time are available online as AVI files (Movies 1, 2; *http://radiology.rsnajnls.org/cgi/content/full/249/1/32/DC1*).

Figure 12

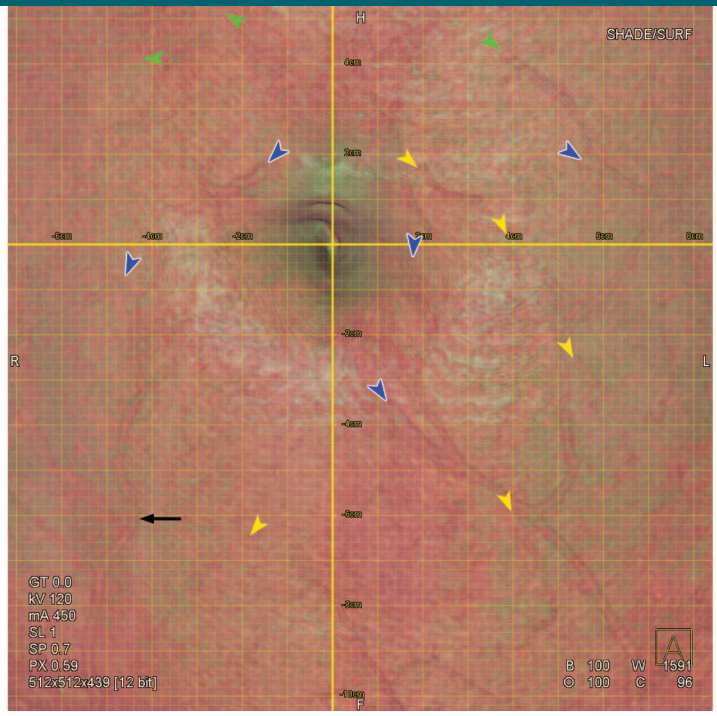

Figure 12: Step 3 of surgical map creation. Anterior volume cropping is disabled, allowing a realistic rendering of the skin surface.

Radiology Report

The key information obtained with abdominal wall CT angiography is documented in the radiology report and distributed to the referring surgeon. The important findings are listed in Table 4. Reconstructed standard axial abdominal images, which are essentially late arterial phase images obtained through the lower abdomen, are also reviewed to exclude gross intraabdominal abnormalities detected within this scanning range. The surgeons at our institution review all images presented to them on the picture archiving and communication system, and they use these images to plan the surgical procedure. Intraoperatively, they use the picture archiving and communication system to view the VRT perforator map to mark the perforators on the patient's abdominal wall with the aid of a ruler and permanent marker pen.

Discussion

Abdominal wall CT angiography is a newly developed technique used for preoperative imaging that may improve the standard of care for autologous breast reconstruction with a free DIEA perforator flap. To our knowledge, Masia et al (17) are the only authors to have related the use of abdominal wall CT angiography to the surgical outcome. In two cohorts of 30 patients in whom the same surgeons performed surgical breast reconstruction with DIEA perforator flaps and *(a)* with preoperative abdominal wall CT angiography in one cohort and *(b)* without preoperative abdominal wall CT angiography in the other cohort, Masia et al (17) reported that the patients who underwent preoperative CT angiography had an average per-patient reduction in surgical time of 100 minutes, one less total flap failure, and one less partial flap necrosis when compared with the patients who did not undergo preoperative CT angiography. They failed to report whether these findings were significant. The anecdotal

experience of our surgeons supports these findings.

In this article, we have described a novel approach to abdominal wall CT angiography that differs substantially from typical abdominal CT angiographic techniques, in that the common femoral artery is used as the site for the bolus trigger, scanning is performed in a caudocranial direction, the automatic exposure control feature is disabled, and a scaled grid overlay tool is used to optimally present information to the surgeons. In our experience with 65 patients, we have had no technical failures, and we have obtained diagnostic-quality images in all patients. We have not observed venous contamination with this technique. Venous contamination potentially would result in a prominent vein being mistaken for a large arterial perforator.

We have not encountered any complications. Use of a common femoral artery bolus trigger site theoretically minimizes the risk of substantial stenotic atherosclerotic aortic disease affecting bolus arrival if an upper abdominal aortic bolus trigger site has been used instead. This bolus trigger site may not prevent substantial stenotic atherosclerotic disease from affecting unilateral common iliac or external iliac arteries, as this might theoretically result in differing arrival times of contrast material within the common femoral arteries. We have not encountered substantial atherosclerotic disease in small or large arteries in any patient. This likely reflects the fact that most patients who undergo breast reconstruction are relatively young and healthy. The oldest patient we examined was 64 years old. This technique has proved accurate in the assessment of three patients who underwent previous extensive abdominal wall surgery and consequently had gross distortion of the normal vascular anatomy, including absence of one or both of the DIEAs. Surgical findings enabled us to confirm the abdominal CT angiography findings and allowed confident planning of abdominal wall flap surgery, with an excellent surgical outcome in these three patients.

We created from scratch a VRT

Figure 13

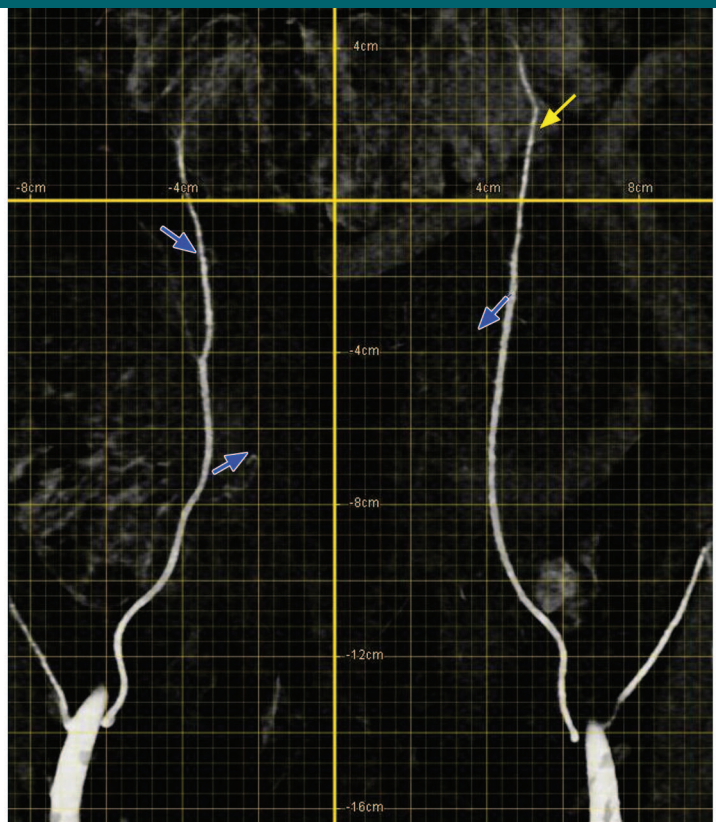

Figure 13: Step 4 of surgical map creation. This image was obtained in a different patient than the one whose image was used for Figures 10–12. The same grid and arrows are overlaid onto the coronal MIP image. For the surgeon, this facilitates a spatial appreciation of the relationship between the perforators and their parent DIEA trunks on a single image. The 0,0 point of the grid marks the umbilicus.

Table 4

Information Obtained with Abdominal Wall CT Angiography and the Image Display, Reconstruction, and Reformation Technique That Best Demonstrates These Findings

Information Obtained with Abdominal Wall CT Angiography	Images That Best Demonstrate These Features*
Branching pattern of the DIEAs (type I, II, or III)	Coronal MIP image
Number and location of large perforators	Manipulated VRT image display, grid maps created from manipulated VRT image display
Caliber of large (>1.0-mm diameter) perforators	Multiplanar reformations, thick axial MIPs
Intramuscular segments of large perforators	Thick axial MIPs
Subfascial segments of large perforators	Thick axial MIPs, manipulated VRT image display
Subcutaneous segments of perforators	Thick axial MIPs, manipulated VRT image display
Anterior rectus sheath and musculotendinous insertions	Manipulated VRT image display
Caliber and course of the superficial inferior epigastric artery	Multiplanar reformations, thick axial MIPs, manipulated VRT image display

* Data are taken from our anecdotal experience.

CLUT that was specifically tailored to abdominal wall CT angiography on the basis of the attenuation of *(a)* contrast material in the DIEA and its branches, *(b)* muscle of the rectus sheath, and *(c)* subcutaneous fat. Contrasting colors (red and green) were chosen. This CLUT enables one to quickly identify the location where the perforators penetrate the anterior rectus sheath when clip planes are used (average reporting time, 7 minutes). Clip planes are necessary, as the skin is not transparent with this VRT CLUT. We have no data to show that the VRT CLUT is more or less accurate than vendor-provided CLUTs; however, we noted that reporting times were at least halved in several cases in which the experience with this newly created CLUT was comparable with that with several vendor-provided CLUTs that were compared side by side in the same patient data sets. We have not used other VRT CLUTs since. While use of this VRT technique is straightforward, we have become aware of several potential pitfalls. Heavy abdominal wall scarring can be both distracting and misleading. In these situations, frequent referral to the axial MIP images is required. This is also required to discern vessels that run within scars. Another potential pitfall is differentiating a perforator with a subfascial segment from one that perforates the anterior rectus sheath and subsequently courses superficially along it. This is important to differentiate, as it could lead to incorrect localization of rectus sheath perforation. Again, this is overcome by referring to axial MIPs, image data, or both.

The most serious drawback of abdominal wall CT angiography is the use of ionizing radiation, particularly in a population that is already at risk. Doppler US and color duplex US have been used with some success in planning perforator flap surgery (37–39). However, this is a technically challenging and time-consuming process that requires experienced sonographers with a good understanding of DIEA perforator flap surgery (17). This was the experience at our institution, and our surgeons abandoned preoperative US in favor of abdominal wall CT angiography early in our experience, despite misgivings about the use of ionizing radiation. Giunta et al (39) reported a high rate of false-positive findings with use of Doppler US (17). To our knowledge, there have been no large head-to-head comparisons of US and abdominal wall CT angiography for preoperative perforator flap planning. In a recent report of eight patients who underwent DIEA perforator surgery, researchers compared preoperative Doppler US with abdominal wall CT angiography and found that US could not be used to detect perforators or to identify DIEA anatomic variations, whereas CT angiography could be used to identify 22 perforators with 100% specificity (23).

High-spatial-resolution magnetic resonance (MR) angiography has the potential to provide results similar to those provided by abdominal wall CT angiography; however, MR angiography has the advantage of not exposing patients to ionizing radiation. Kelly et al (40) report high sensitivity for use of MR angiography in planning free fibula flap reconstructive surgery. To our knowledge, there have been no reports of abdominal wall MR angiography. Our own preliminary experience with abdominal wall MR angiography (three patients were examined with a 1.5-T system and three were examined with a 3-T system) has been mixed. Reproducibility has been poor, and the depiction of smaller perforators has been disappointing.

In this article, we have defined the segmental anatomy of the anterior musculocutaneous perforating branches of the DIEA and discussed the importance of these features in pre- and intraoperative surgical planning and technique. The acquisition protocol and postprocessing, image reconstruction, and reading techniques we have formulated are optimized to obtain comprehensive anatomic information while minimizing radiation dose to the patient. Its anatomic accuracy has been reported in several preliminary cadaveric and surgical studies (17–23). To our knowledge, no large prospective study has been performed. The detailed description provided will allow other radiologists and surgeons interested in free DIEA perforator flap surgery to incorporate this useful tool into their practice.

Acknowledgments: We thank Francesco Gaillard, MBBS, PG Dip Surg Anat, Royal Melbourne Hospital, for the three-dimensional illustration of perforator anatomy; Francesca Langenberg, DCR, The Royal Melbourne Hospital, for assistance with acquisition and postprocessing CT protocols; and Paul Einsiedel BSc (Hons), The Royal Melbourne Hospital, for performing CT dosimetry.

References

1. Holmström H. The free abdominoplasty flap and its use in breast reconstruction: an experimental study and clinical case report. Scand J Plast Reconstr Surg 1979;13:423–427.
2. Granzow JW, Levine JL, Chiu ES, et al. Breast reconstruction with perforator flaps. Plast Reconstr Surg 2007;120:1–12.
3. Nahabedian MY, Momen B, Galdino G, et al. Breast reconstruction with the free TRAM or DIEP flap: patient selection, choice of flap, and outcome. Plast Reconstr Surg 2002;110:466–475.
4. Garvey PB, Buchel EW, Pockaj BA, et al. DIEP and pedicled TRAM flaps: a comparison of outcomes. Plast Reconstr Surg 2006;117:1711–1719.
5. Bajaj AK, Chevray PM, Chang DW. Comparison of donor-site complications and functional outcomes in free muscle-sparing TRAM flap and free DIEP flap breast reconstruction. Plast Reconstr Surg 2006;117:737–746.
6. Schaverien MV, Perks AG, McCulley SJ. Comparison of outcomes and donor-site morbidity in unilateral free TRAM versus DIEP flap breast reconstruction. J Plast Reconstr Aesthet Surg 2007;60:1219–1224.
7. Gill PS, Hunt JP, Guerra AB, et al. A 10-year retrospective review of 758 DIEP flaps for breast reconstruction. Plast Reconstr Surg 2004;113:1153–1160.
8. Blondeel PN. One hundred free DIEP flap breast reconstructions: a personal experience. Br J Plast Surg 1999;52:104–111.
9. Blondeel N, Vanderstraeten GG, Monstrey SJ, et al. The donor site morbidity of free DIEP flaps and free TRAM flaps for breast reconstruction. Br J Plast Surg 1997;50:322–330.
10. Allen RJ. DIEP versus TRAM for breast reconstruction. Plast Reconstr Surg 2003;111:2478.

11. Kaplan JL, Allen RJ. Cost-based comparison between perforator flaps and TRAM flaps for breast reconstruction. Plast Reconstr Surg 2000;105:943–948.

12. Allen RJ. Comparison of the costs of DIEP and TRAM flaps. Plast Reconstr Surg 2001; 108:2165.

13. Spiegel AJ, Khan FN. An intraoperative algorithm for use of the SIEA flap for breast reconstruction. Plast Reconstr Surg 2007; 120:1450–1459.

14. Holm C, Mayr M, Höfter E, et al. The versatility of the SIEA flap: a clinical assessment of the vascular territory of the superficial epigastric inferior artery. J Plast Reconstr Aesthet Surg 2007;60:946–951.

15. Moon HK, Taylor GI. The vascular anatomy of rectus abdominus musculocutaneous flaps based on the deep superior epigastric system. Plast Reconstr Surg 1988;82:815–832.

16. Lindsey JT. Integrating the DIEP and muscle-sparing (MS-2) free TRAM techniques optimizes surgical outcomes: presentation of an algorithm for microsurgical breast reconstruction based on perforator anatomy. Plast Reconstr Surg 2007;119:18–27.

17. Masia J, Clavero JA, Larranaga JR, et al. Multidetector-row computed tomography in the planning of abdominal perforator flaps. J Plast Reconstr Aesthet Surg 2006;59:594–599.

18. Alonso-Burgos A, García-Tutor E, Bastarrika G, et al. Preoperative planning of deep inferior epigastric artery perforator flap reconstruction with multislice-CT angiography: imaging findings and initial experience. J Plast Reconstr Aesthet Surg 2006;59:585–593.

19. Rosson GD, Williams CG, Fishman EK, et al. 3D CT angiography of abdominal wall vascular perforators to plan DIEAP flaps. Microsurgery 2007;27:641–646.

20. Rozen WM, Phillips TJ, Ashton MW, et al. Pr15 The branching pattern of the DIEA for perforator flaps: the importance of preoperative CT angiography. ANZ J Surg 2007;77: A65.

21. Rozen WM, Phillips TJ, Ashton MW, et al. Pr11 preoperative imaging for DIEA perforator flaps: a comparative study of CT angiography and Doppler ultrasound. ANZ J Surg 2007;77:A64.

22. Rozen WM, Stella DL, Ashton MW, et al. Three-dimensional CT angiography: a new technique for imaging microvascular anatomy. Clin Anat 2007;20:1001–1003.

23. Rozen WM, Phillips TJ, Ashton MW, et al. Preoperative imaging for DIEA perforator flaps: a comparative study of computed tomographic angiography and Doppler ultrasound. Plast Reconstr Surg 2008;121:9–16.

24. Tregaskiss AP, Goodwin AN, Acland RD. The cutaneous arteries of the anterior abdominal wall: a three-dimensional study. Plast Reconstr Surg 2007;120:442–450.

25. Boyd JB, Taylor GI, Corlett R. The vascular territories of the superior epigastric and the deep inferior epigastric systems. Plast Reconstr Surg 1984;73:1–16.

26. Vandevoort M, Vranckx JJ, Fabre G. Perforator topography of the deep inferior epigastric perforator flap in 100 cases of breast reconstruction. Plast Reconstr Surg 2002; 109:1912–1918.

27. Awai K, Takada K, Onishi H, et al. Aortic and hepatic enhancement and tumor-to-liver contrast: analysis of the effect of different concentrations of contrast material at multidetector row helical CT. Radiology 2002; 224:757–763.

28. Cademartiri F, Mollet NR, van der Lugt A, et al. Intravenous contrast material administration at helical 16-detector row CT coronary angiography: effect of iodine concentration on vascular attenuation. Radiology 2005;236:661–665.

29. Chawla S. Advances in multidetector computed tomography: applications in neuroradiology. J Comput Assist Tomogr 2004; 28(suppl 1):S12–S16.

30. Fenchel S, Fleiter TR, Aschoff AJ, et al. Effect of iodine concentration of contrast media on contrast enhancement in multislice CT of the pancreas. Br J Radiol 2004;77: 821–830.

31. Schoellnast H, Deutschmann HA, Fritz GA, et al. MDCT angiography of the pulmonary arteries: influence of iodine flow concentration on vessel attenuation and visualization. AJR Am J Roentgenol 2005;184:1935–1939.

32. Mulkens TH, Bellinck P, Baeyaert M, et al. Use of an automatic exposure control mechanism for dose optimization in multi-detector row CT examinations: clinical evaluation. Radiology 2005;237:213–223.

33. Berg MH, Manninen HI, Vanninen RL, et al. Assessment of renal artery stenosis with CT angiography: usefulness of multiplanar reformation, quantitative stenosis measurements, and densitometric analysis of renal parenchymal enhancement as adjuncts to MIP film reading. J Comput Assist Tomogr 1998;22: 533–540.

34. Brink JA, Lim JT, Wang G, et al. Technical optimization of spiral CT for depiction of renal artery stenosis: in vitro analysis. Radiology 1995;194:157–163.

35. Hyde DE, Habets DF, Fox AJ, et al. Comparison of maximum intensity projection and digitally reconstructed radiographic projection for carotid artery stenosis measurement. Med Phys 2007;34:2968–2974.

36. Van Hoe L, Vandermeulen D, Gryspeerdt S, et al. Assessment of accuracy of renal artery stenosis grading in helical CT angiography using maximum intensity projections. Eur Radiol 1996;6:658–664.

37. Mah E, Temple F, Morrison W. Value of pre-operative Doppler ultrasound assessment of deep inferior epigastric perforators in free flap breast reconstruction. ANZ J Surg 2005;75(S1):A89.

38. Hallock GG. Doppler sonography and color duplex imaging for planning a perforator flap. Clin Plast Surg 2003;30:347–357.

39. Giunta RE, Geisweid A, Feller AM. The value of preoperative Doppler sonography for planning free perforator flaps. Plast Reconstr Surg 2000;105:2381–2386.

40. Kelly AM, Cronin P, Hussain HK, et al. Preoperative MR angiography in free fibula flap transfer for head and neck cancer: clinical application and influence on surgical decision making. AJR Am J Roentgenol 2007;188:268–274.